Investigation of Parallel Manipulators Using Linear Complex Approximation

A. Wolf
e-mail: Alon.wolf@cmu.edu

M. Shoham
e-mail: shoham@tx.technion.ac.il

Robotics Laboratory,
Department of Mechanical Engineering,
Technion—Israel Institute of Technology
Haifa 32000, Israel

This investigation deals with singularity analysis of parallel manipulators and their instantaneous behavior while in or close to a singular configuration. The method presented utilizes line geometry tools and screw theory to describe a manipulator in a given position. Then, this description is used to obtain the closest linear complex, presented by its screw coordinates, to the set of governing lines of the manipulator. The linear complex axis and pitch provide additional information and a better physical understanding of the type of singularity and the motion the manipulator tends to perform in a singular point and in its neighborhood. Examples of Hunt's, Fichter's and 3-UPU singularities, along with a few selected examples taken from Merlet's work [1], are presented and analyzed using this method. [DOI: 10.1115/1.1582876]

1 Introduction

Numerous investigations have been conducted on singular configurations of mechanisms, with recent emphasis on parallel manipulators. When dealing with parallel robots, the identification of singular configurations is of greater importance because while in such a configuration the mechanism loses its stiffness and gains extra degrees of freedom [2,3]. Physically, it means that the structure cannot resist or balance an external wrench applied at the moving platform, which might lead to a general failure of, or permanent damage to, the manipulator and surrounding equipment. This is why singularity analysis of parallel robots and singularity-free workspace, e.g. [4], is one of the most important and one of the earliest steps in the robot design procedure.

The identification of singular configurations has been approached from different points of view. In [5], the authors introduced three kinds of singularities, all based on the vanishing of the Jacobian matrix determinant. Further interpretation of the method is given in [6]. Singularity classification into three categories: architecture, configuration, and formulation, is presented in [7–9]. Their algorithm consists also of the velocity-equation formulation which is a Jacobian matrix determinant based approach. In [3], the authors studied the singularity loci of the Gough-Stewart platform, and obtained a graphical representation of these loci in the manipulator workspace. The algorithm used is based on deriving expressions of the determinant of the Jacobian matrix using the linear decomposition method and co-factor expansion. More studies have been conducted on deriving the analytical expressions of the singularity loci for planar and spherical parallel manipulators, see [10–12].

Several numerical procedures to overcome the complexity involved in the singularity loci analytical expression have also been developed, e.g., [13,14].

The above-mentioned investigations are examples taken from a large body of literature, that use the Jacobian matrix to determine the manipulator's singular configurations. However, less emphasis is placed on the behavior of the manipulator while being at these points.

A different approach to determining the self-motion of parallel mechanisms based on geometrical insight is suggested in [15]. The algorithm uses the Lie group representation of space congruences and the quadratic constraint, which describes the conditions governing a point on the moving platform to move on a sphere. A list of all degenerated parallel manipulators that are architecturally singular is presented in [16].

Line geometry tools were also used to investigate singular configurations of parallel manipulators. Using Plücker's line coordinates and Grassman line geometry Merlet [17], showed that the robot's Jacobian matrix, composed of Plücker line coordinates, has a lower rank if its columns are linearly dependent. In a later work, [18] he determined all the constraint equations of the position parameters using line geometry. With this method, the motion performed by the manipulator in singular configurations could be determined numerically and analytically. Fichter [19], analyzed the singular configurations of a Gough-Stewart platform, in which the legs exert pure forces, by looking for configurations where their lines of action are linearly dependent. Using this approach, he found that singularity occurs whenever the moving platform rotates about a normal to the base platform by 90 deg. Collins and Long [20] showed that columns of the Jacobian matrix are zero-pitch wrenches (lines) acting on the moving platform. The authors illustrated how line geometry and rank-determining geometric construction could be used to obtain all singular configurations. Based on Dandurand's work [21], which investigated line variety and line dependence, Ben-Horin [22], determined the singularity configurations of 17 Gough-Stewart type platforms. Simaan and Shoham [23], used line geometry tools to investigate the singularity of a class of non-fully parallel manipulators that share the same instantaneous direct kinematic matrix.

Hao and McCarthy [24] used screw theory to investigate the geometrical conditions for singular configurations in parallel mechanisms that are also related to line dependency conditions. Huang et al. [25], analyzed the general linear complex of the 3-3 and 3-6 SPT (Spherical, Prismatic, Universal) parallel mechanisms, and provided the geometrical conditions for their singularities for several geometries of the robots' platforms.

The present investigation utilizes line geometry and screw theory to determine the singular configurations of parallel manipulators as well as their behavior at these points. A 6×6 matrix is derived, even for robots with fewer that six DOF (Degrees Of Freedom), that captures the actuators' and the constraints' governing lines of action. Using this description, and an algorithm presented by Pottmann et al. [26], the closest linear complex to these lines is obtained. The closest linear complex, described by its axis and pitch, provides additional information on the manipulator's instantaneous motion and understanding of the type of singularity when the manipulator is at, or in the neighborhood of, a singular configuration.

Contributed by the Mechanisms and Robotics Committee for publication in the JOURNAL OF MECHANICAL DESIGN. Manuscript received Nov. 2001; rev. Nov. 2002. Associate Editor: G. S. Chirikjian.

2 Linear Complex Approximation Algorithm—LCAA

This section presents a short summery of the algorithm developed by Pottmann et al. [26]. Given k lines, L_i, by their Plücker line coordinates,

$$L_i=(l_i,\overline{l_i}) \quad i=1,\ldots,k \ \ (k\geqslant 6) \tag{1}$$

this algorithm determines the linear complex $C(c,\overline{c})$, which is the closest one to the given set of lines L_i. The linear complex C, is not necessarily located on the Klein quadric [27] meaning that $c\cdot\overline{c}$ (dot product) is not necessarily equal to zero. For more information and further interpretation of the linear complex, we refer the reader to Pottmann et al. [26].

According to Klein [27], the moment of a line, L_i, with respect to a linear complex C is given by:

$$m(L,C)=\frac{|\overline{c}\cdot l_i+c\cdot\overline{l_i}|}{\|c\|} \tag{2}$$

Hence, given a set of lines L_i, the closest linear complex among all linear complexes χ can be given by the minimization of:

$$\sum_{i=1}^{k} m(L_i,\chi)^2 \tag{3}$$

where χ is given by $\chi=(x,\overline{x})\in IR^6$

Eq. (3) is equivalent to minimizing the following positive semidefinite quadratic form, over χ:

$$F(X)=\sum_{i=1}^{k}(\overline{x}\cdot l_i+x\cdot\overline{l_i})^2=\chi^T M\chi \tag{4}$$

under the normalization condition $1=\|x\|^2=\chi^T D\chi$, where $D=\mathrm{diag}(1,1,1,0,0,0)$.

Writing L_i in axis coordinates as $L_{a,i}=(\overline{l_{a,i}},l_{a,i})$, then M in Eq. (4) is given as (also known as the Gramian matrix):

$$M=\sum_{i=1}^{k} L_{a,i}\cdot L_{a,i}^T \tag{5}$$

Eq. (4) is a general eigenvalue problem. Using Lagrange multipliers λ_i, one obtains:

$$(M-\lambda_i D)\cdot\chi=0, \quad x^T Dx=1 \tag{6}$$

Hence, λ is the root of the equation:

$$\det(M-\lambda_i D)=0 \tag{7}$$

Defining $1/\lambda_i=\xi_i$, Eq. (7) becomes:

$$\det(\xi_i M-D)=0 \tag{8}$$

Multiplying by M^{-1}:

$$\det(\xi_i I-M^{-1}D)=0 \tag{9}$$

Since three diagonal elements of D are zero, Eq. (9) results in a cubic equation in ξ, where all ξ_i are the eigenvalues of $M^{-1}D$, and χ_i are its corresponding eigenvectors (for the basic problem Eq. (7), $\lambda_i=1/\xi_i$).

For any root λ_i and corresponding eigenvector $\chi_i=(x_i,\overline{x_i})$, which is the solution of (6), one gets:

$$F(X)=\chi_i^T M\chi_i=\lambda_i\chi_i^T D\chi_i=\lambda_i \tag{10}$$

Hence, all roots are non-negative, and the solution, C, is the eigenvector χ_i corresponding to the smallest eigenvalue λ_i.

Given the lines $L_i=(l_i,l_i)$ and the closest linear complex C, the standard deviation of the lines from C is given by:

$$\sigma=\sqrt{\frac{\lambda_i}{k-5}} \tag{11}$$

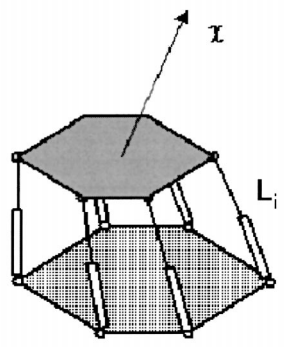

Fig. 1 Gough-Stewart platform, the lines L_i and the resulting twists

Moreover, given the closest linear complex found by the algorithm, the axis, A, of the linear complex is given by:

$$A(a,\overline{a})=(c,\overline{c}-p\cdot c) \tag{12}$$

where p is its pitch given by:

$$p=\frac{c\cdot\overline{c}}{c^2} \tag{13}$$

When solving Eq. (7) two small eigenvalues might be revealed, meaning that there are two solutions for C, (C_1,C_2), that are almost equally good. Hence, the lines L_i can be well approximated by the lines of the intersection of the two linear complexes: $C_1\cap C_2$ (this is a two-parameter family of lines—a linear congruence). Analogously, three small eigenvalues λ_1, λ_2, λ_3 define three linear complexes (a bundle of complexes). The intersection forms a one-parameter family of lines such as a regulus, a pair of lines, a union of lines, or a whole plane.

3 Applications of the Linear Complex Approximation Algorithm and Examples

It has been shown by Merlet [1], and Husty and Karger [16], that for a parallel robot with $k\geqslant 6$ (k being the number of robot limbs), the robot is in a singular configuration if and only if the lines along the limbs lie in a linear complex. As shown in the following example this result can also be obtained for a robot with fewer than six DOF when both the actuation and constraints forces are considered.

The minimization procedure shown in section 2 minimizes the reciprocal product [28,25] of the wrench applied on the moving platform and the twists. This yields the work generated by the wrench to a body instantaneously undergoing a twist deformation. In the case of parallel manipulators this is interpreted as the minimization of the instantaneous work generated by a set of wrenches, given by L_i, acting on a body instantaneously moving in a twist direction given by χ. If a wrench is acting on a rigid body such that it produces no work while the body is undergoing an infinitesimal twist, the two are assumed to be reciprocal to each other and their reciprocal product is zero. This is the case in a singular configuration of the robot.

Consider the Gough-Stewart platform shown in Fig. 1. The rows of the Jacobian matrix of the manipulator are composed of the Plücker coordinates of the wrenches acting along its limbs L_i [29,30].

Applying the Linear Complex Approximation Algorithm to this set of wrenches while the platform is moving instantaneously along the twist direction given by χ, the smallest λ_i determines the direction along which the work generated by the set of wrenches is minimal. When the reciprocal product is zero, there is no work generated by the set of wrenches when the platform moves in the twist direction given by χ. We use this physical

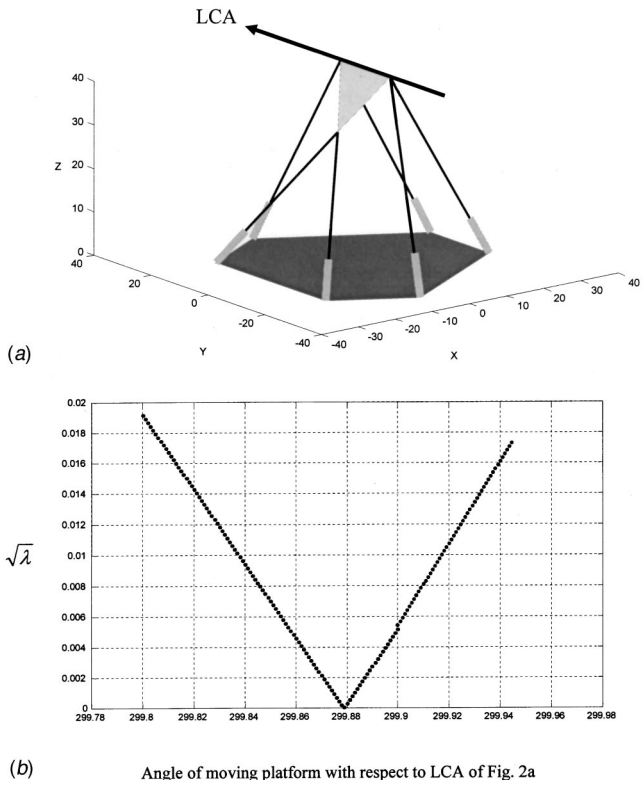

Fig. 2 (*a*) Hunt's singularity—two limbs and the moving platform are coplanar; (*b*) $\sqrt{\lambda}$ as function of the moving, platform rotation angle, α, about the LCA axis of Fig. 2(*a*)

interpretation of the reciprocal product of screws in order to investigate the behavior of a given robotics structure in a given configuration.

3.1 Example 1: Hunt's Singularity. This example demonstrates a 6−3 Gough-Stewart platform while in Hunt's singularity, i.e. the platform and two limbs are in one plane. In this case, all six lines along the limbs intersect one line, denoted as LCA (linear complex axis) shown as a thick black line in Fig. 2(*a*) and hence the robot is in a singular configuration of a linear complex. Simulation results of a robot with a base radius of 0.3 and platform radius of 0.1 are shown in Figs. 2(*a*,*b*):

Hunt's singularity occurs when all six lines L_i intersect one line denoted as LCA in Fig. 2(*a*). This line passes through the upper edge (connecting two joints) of the triangle-shaped moving platform. Applying the LCAA results in a linear complex whose axis is along this line with a zero pitch and the magnitude of λ is zero. This means that this configuration is singular and the platform is able to execute free instantaneous rotation about an axis through the platform upper edge.

This example reveals that when using LCAA one can gain a better understanding of Hunt's singularity by finding both the axis of rotation and the instantaneous uncontrolled screw motion (direction and pitch) of the moving platform.

3.2 Example 2: Fichter's Singularity. This example shows a 6−6 Gough—Stewart platform moving through Fichter's singularity (90 deg rotation of the moving platform about the vertical axis while the moving platform is horizontal). Simulation results for a robot with a base radius of 0.3 and platform radius of 0.1 are given in Figs. 3(*a*–*d*):

In Fichter's singularity, the platform gains an extra DOF, which is a screw motion about the *z*-axis. The axis of the linear complex is given in Figs. 3(*a*) and 3(*b*) (denoted as LCA). Fig. 3(*c*) presents the values of $\sqrt{\lambda_{\min}}$ in this singular configuration and its neighborhood, whose corresponding linear complex axis is shown in Figs. 3(*a*,*b*). Notice that graph 3(*c*) shows a zero value at 90 deg rotation (where singularity occurs) which corresponds to a non-zero pitch value of the linear complex; hence at this singularity the moving platform performs a screw motion of rotation and translation around the linear complex axis.

3.3 Example 3: Singular Configuration of Type 3c. This example depicts the TSSM (Triangular Simplified Symmetric Manipulator) taken from Merlet [17].

The 3(*c*) singularity occurs when four limbs of the manipulator intersect at a common point. Observing the robot structure, one can see that pairs of two limbs intersect at a spherical joint of the moving platform. Hence, one option to have four lines intersect at one point is shown in Fig. 5.

The LCAA results in a zero-pitch linear complex (LCA) with $\lambda=0$, meaning that the robot is in a singular configuration and can instantaneously rotate (pure rotation) around the linear complex axis. Vertex B1 of the platform serves as the vertex of a bundle of lines 1, 2, 3 and 5 along limbs 1, 2, 3 and 5, respectively. In this configuration, the platform center P is located at: $P=[0.317\ 0.069\ 0.325]$ with orientation angles of $\psi=45$ deg, $\theta=50$ deg, $\phi=0$ deg.

3.4 Example 4: Singular Configuration of Type 4d. This example deals with the TSSM manipulator (Fig. 4) presented by Merlet [17]. This singular configuration produces a line variety of dimension four, called linear congruence where five lines along the manipulator's limbs intersect two lines. Due to the manipulator structure, pairs of limbs lie in a plane. Hence, a line that lies in one of these planes and crosses the spherical joint of another pair intersects four limbs. In a case that one of the limbs of the third pair crosses the same spherical joint it results in five lines that intersect two lines and hence a singular configuration. This configuration is depicted in Figs. 6(*a*) and 6(*b*) where limbs 1, 2, 4, 5 and 6 intersect line LCA1 and LCA2.

Simulation of this configuration results in a zero-pitch linear complex with $\sigma=0$, meaning that the robot is in a singular configuration and can instantaneously rotate (pure rotation) around the linear complex axis. In this configuration, P (center of platform) is located at: $P=[0.076,-0.162,0.238]$ and $\psi=12$ deg, $\theta=60$ deg, $\phi=54$ deg.

4 Analysis of the 3-UPU Robot Using LCAA

The 3-DOF, 3-UPU robot was introduced by Lung-Wen Tsai in 1996 [31]. This robot is composed of two platforms (base and mobile) connected by three identical kinematic chains. Each chain comprises a prismatic actuator with two universal joints at its ends. There are several arrangements of the upper and lower universal joints, one of which is presented in Fig. 7(*a*). However, in our report, we investigate the SNU robot (Seoul National University) given in Fig. 7(*b*), whose universal joint arrangement is given in Fig. 9. (see also the investigation of Di Gregorio and Parenti-Castelli [32], which presents a solution to the singularity conditions that can be extended to various arrangements of the universal joints).

When deriving the Jacobian matrix of the 3-UPU using the screw-based Jacobian method [33], the result is a 6×3 Jacobian matrix because of the three DOF of the manipulator. However, in order to obtain a full 6×6 Jacobian matrix of the robot, including the moments of constraints, one can express the set of static equilibrium conditions of the upper platform. These expressions result in a 6×6 Jacobian matrix that maps the external wrench acting on the moving platform to the moments of the internal forces that are generated by the robotic structure on the moving platform.

Starting with the screw-based Jacobian method, consider the 3-UPU robotic structure in Figs. 7(*b*) and 8. The Jacobian matrix of the manipulator is composed of the three screws along its limbs. These screws are the reciprocal screws to all the passive joint screws in each limb [30,33]. In order to define the Jacobian

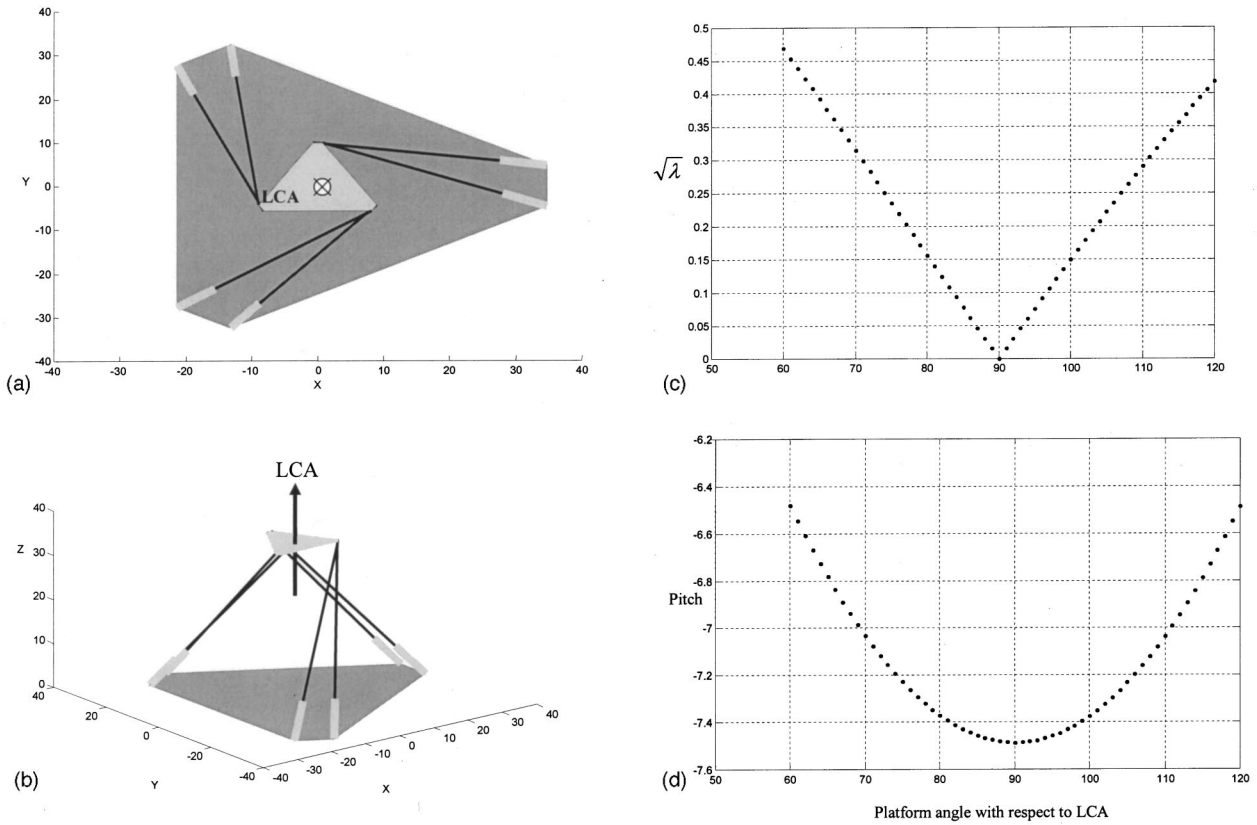

Fig. 3 (*a*) **Fichter's singularity—90 deg rotation of the moving platform about the *Z* axis, top views;** (*b*) **Fichter's singularity—90 deg rotation of the moving platform, from home position, about the *Z* axis: isometric views;** (*c*) $\sqrt{\lambda}$ **as a function of the moving platform rotation angle about the *Z* axis.** (*d*) **Values of the closest linear complex's pitch as a function of the moving platform rotation angle about the *Z* axis.**

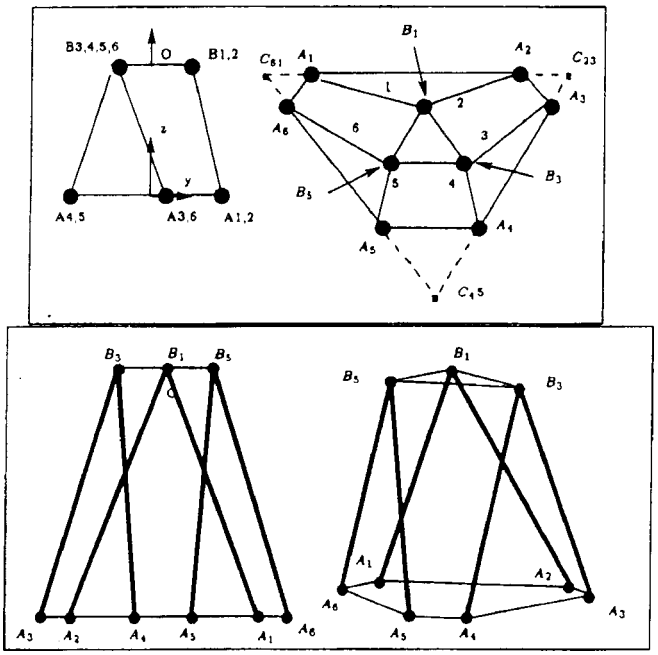

Fig. 4 The TSSM Manipulator, Merlet [17]

matrix, it is necessary to describe all five joint screws of the manipulator. Note that the only actuated joint in each limb is the third and that the rest are passive.

Let $s_{j,i}$ be a unit vector along the *j*th joint axis of the *i*th limb. Then, one can denote the five unit screws of each limb as (see Fig. 8):

$$\$_{1,i}=\begin{bmatrix} s_{1,i} \\ (b_i-d_i)\times s_{1,i} \end{bmatrix} \tag{14}$$

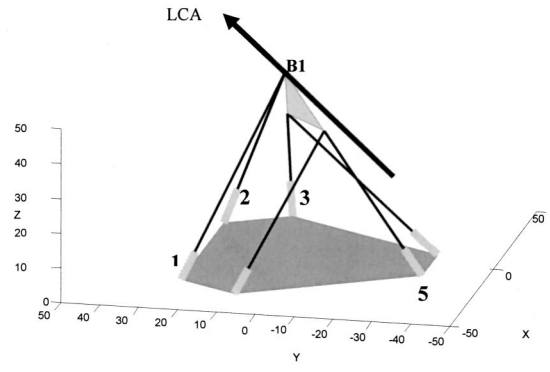

Fig. 5 Type 3c singularity with four line-1,2,3,5-intersect at vertex B1

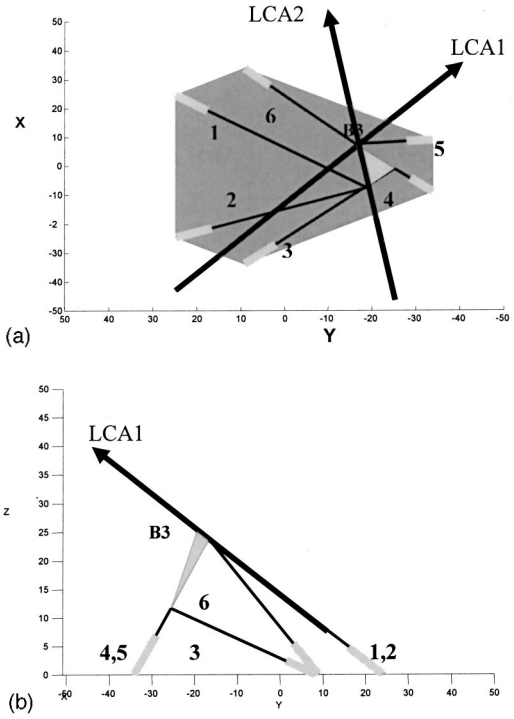

Fig. 6 (*a*) Type 4d singularity where lines LCA1 and LCA2 cross the plane spanned by L1 and L2, vertex B3 joining L5 and L6 and intersect a line along limb 4: top view; (*b*) Type 4d singularity (LCA2 not shown for clarity): side view.

$$\hat{\$}_{2,i}=\begin{bmatrix} s_{2,i} \\ (b_i-d_i)\times s_{2,i} \end{bmatrix} \tag{15}$$

$$\hat{\$}_{3,i}=\begin{bmatrix} 0 \\ s_{3,i} \end{bmatrix} \tag{16}$$

$$\hat{\$}_{4,i}=\begin{bmatrix} s_{4,i} \\ b_i\times s_{4,i} \end{bmatrix} \tag{17}$$

$$\hat{\$}_{5,i}=\begin{bmatrix} s_{5,i} \\ b_i\times s_{5,i} \end{bmatrix} \tag{18}$$

where $b_i=\overline{PB_i}$, $d_i=\overline{A_iB_i}=d_i s_{3,i}$, and $\hat{\$}_{3,i}$ is a prismatic join with infinite pitch.

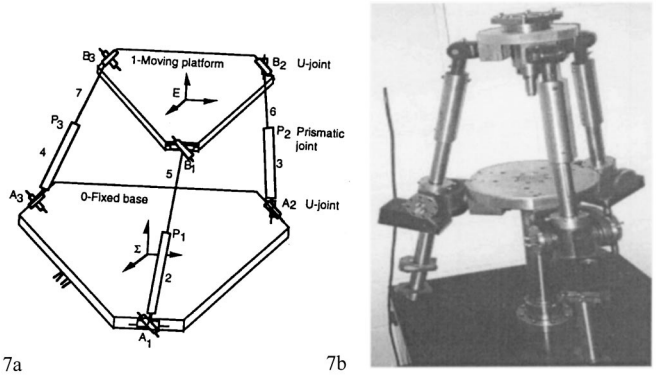

7a 7b

Fig. 7 (*a*) A 3-DOF 3-UPU parallel manipulator [31]; (*b*) A 3-DOF 3-UPU parallel manipulator (SNU)

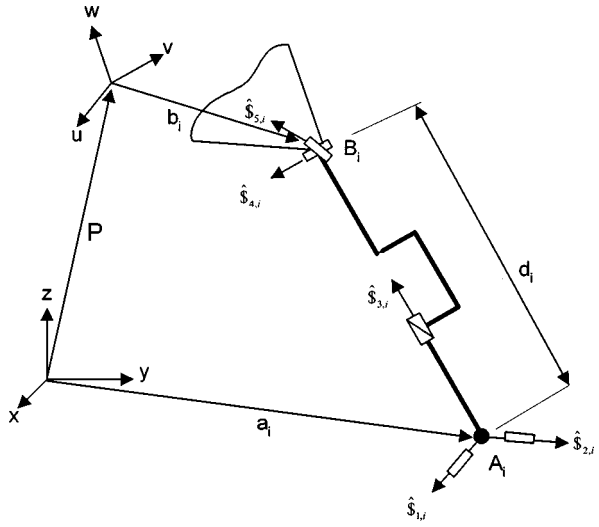

Fig. 8 Equivalent kinematic structure of the UPU robot's limb

When expressing the instantaneous twist of the moving platform in terms of the joint screws and regarding each limb as an open-loop chain, one obtains [33]:

$$\$_p=\dot{\theta}_1\hat{\$}_{1,i}+\dot{\theta}_2\hat{\$}_{2,i}+\dot{d}_3\hat{\$}_{3,i}+\dot{\theta}_4\hat{\$}_{4,i}+\dot{\theta}_5\hat{\$}_{5,i}\,. \tag{19}$$

Since the axes of all passive joints in each limb intersect the line passing through points A_i, B_i, a screw that is reciprocal to all the screws is:

$$\hat{\$}_{r3,i}=\begin{bmatrix} s_{3,i} \\ b_i\times s_{3,i} \end{bmatrix}. \tag{20}$$

Define the six screw components as:

$$\$=(S_1,S_2,S_3,S_4,S_5,S_6) \tag{21}$$

Then the reciprocal product of two screws $\$_1$, $\$_2$ is given in [26]:

$$\Omega(\$_1,\$_2)=S_{1,1}S_{2,4}+S_{1,2}S_{2,5}+S_{1,3}S_{2,6}+S_{1,4}S_{2,1}+S_{1,5}S_{2,3}+S_{1,3}S_{2,6} \tag{22}$$

When the two screws are reciprocal, their reciprocal product is zero:

$$\Omega(\$_1\$_2)=0. \tag{23}$$

Taking the reciprocal product of both sides of $\$_p$ with $\hat{\$}_{r3,i}$ according to (22), one obtains:

$$\Omega(\hat{\$}_{r3,i}\$_p)=\dot{d}_i \quad \text{for } i=1,2,3 \tag{24}$$

Writing this for each limb one obtains:

$$J_x\dot{x}=J_q\dot{q}, \tag{25}$$

where

$$J_x=\begin{bmatrix} (b_1\times s_{3,1})^T & s_{3,1}^T \\ (b_2\times s_{3,2})^T & s_{3,2}^T \\ (b_3\times s_{3,3})^T & s_{3,3}^T \end{bmatrix}$$

$$J_q=I(3\times 3 \text{ identity matrix}) \tag{26}$$

$$\dot{x}=[\omega_x,\omega_y,\omega_z,v_{px},v_{py},v_{pz}]$$

$$\dot{q}=[\dot{d}_1,\dot{d}_2,\dot{d}_3]$$

Taking $\dot{x}$ to be the velocity of the moving platform, and $\dot{q}$ as the vector of actuator joint rates, one can define the relation using J_x.

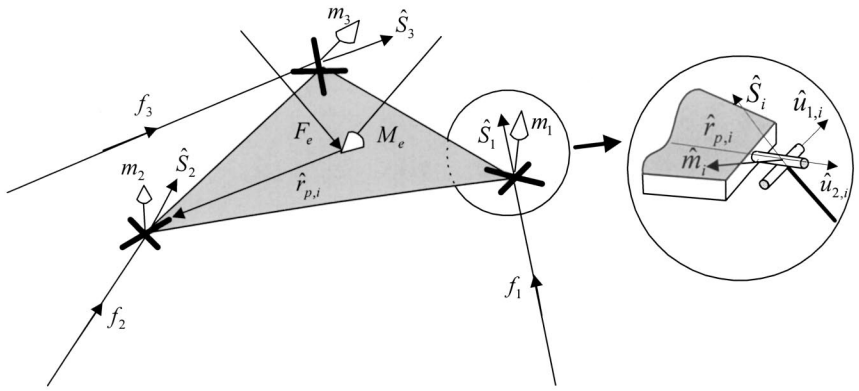

Fig. 9 Force and moment transmitted to the moving platform

In order to obtain the full 6×6 Jacobian matrix that maps the external wrench to internal joints' reactions, the static equilibrium condition of the moving platform is derived as (Fig. 9):

$$\sum_{i=1}^{3} f_i \hat{S}_i - F_e = 0$$
$$\sum_{i=1}^{3} m_i \hat{U}_i + \sum_{i=1}^{3} {}^{w}R_P \cdot \hat{r}_{p,i} \times f_i \cdot \hat{S}_i - M_e = 0 \tag{27}$$

where $\hat{U}_i$ is a unit vector normal to the two axes of the upper U joint of limb i. Observing Fig. 9, $\hat{u}_{2,i}$ is a unit vector along the first pair of the U joint (connected to the platform), and its direction is along $\hat{r}_{pi}$ (in platform coordinates). $\hat{u}_{1,i}$ is a unit vector along the second pair of the U joint (connected to limb i), and $\hat{S}_i$ is a unit vector along limb i. Due to the U joint structure, $\hat{u}_{1,i}$ is perpendicular to both $\hat{u}_{2,i}$ and $\hat{S}_i$, and hence:

$$\hat{u}_{1,i} = \frac{\hat{u}_{2,1} \times \hat{S}_i}{|\hat{u}_{2,1} \times \hat{S}_i|} \tag{28}$$

Substituting $\hat{u}_{2,i} = {}^{w}R_p \cdot \hat{r}_{p,i}$ yields:

$$\hat{u}_{1,i} = {}^{w}R_p \cdot \hat{r}_{p,i} \times \hat{S}_i \tag{29}$$

${}^{w}R_p$ is a rotation matrix from the platform coordinate system to the world coordinate system. Defining:

$$\hat{U}_i = \hat{u}_{2,i} \times \hat{u}_{1,i} \tag{30}$$

Substituting Eqs. (28) and (29) to Eq. (30):

$$\hat{U}_i = {}^{w}R_p \cdot \hat{r}_{p,i} \times \left(\frac{{}^{w}R_p \cdot \hat{r}_{p,i} \times \hat{S}_i|}{{}^{w}R_p \cdot \hat{r}_{p,i} \times \hat{S}_i|} \right) \tag{31}$$

Writing Eq. (27) as a matrix yields:

$$\begin{bmatrix} \hat{S}_1 & \hat{S}_2 & \hat{S}_3 & 0 & 0 & 0 \\ {}^{w}R_p \cdot \hat{r}_{p,1} \times \hat{S}_1 & {}^{w}R_p \cdot \hat{r}_{p,2} \times \hat{S}_2 & {}^{w}R_p \cdot \hat{r}_{p,3} \times \hat{S}_3 & \hat{U}_1 & \hat{U}_2 & \hat{U}_3 \end{bmatrix} \times \begin{bmatrix} f_1 \\ f_2 \\ f_3 \\ m_1 \\ m_2 \\ m_3 \end{bmatrix} = \begin{bmatrix} F_e \\ M_e \end{bmatrix} \tag{32}$$

The forces at the robot joints are given by:

$$\begin{bmatrix} \hat{S}_1 & \hat{S}_2 & \hat{S}_3 & 0 & 0 & 0 \\ {}^{w}R_p \cdot \hat{r}_{p,1} \times \hat{S}_1 & {}^{w}R_p \cdot \hat{r}_{p,2} \times \hat{S}_2 & {}^{w}R_p \cdot \hat{r}_{p,3} \times \hat{S}_3 & \hat{U}_1 & \hat{U}_2 & \hat{U}_3 \end{bmatrix}^{T^{-1}} \times \begin{bmatrix} F_e \\ M_e \end{bmatrix} = \begin{bmatrix} f_1 \\ f_2 \\ f_3 \\ m_1 \\ m_2 \\ m_3 \end{bmatrix} \tag{33}$$

Observing Eq. (32) and Eq. (33) knowing that for parallel structures $J^T f = f_e$ or $J^{T^{-1}} f_e = f$, one can detect that the Jacobian matrix, J, for the 3-UPU robot is given by:

$$J = \begin{bmatrix} \hat{S}_1 & \hat{S}_2 & \hat{S}_3 & 0 & 0 & 0 \\ {}^{w}R_p \cdot \hat{r}_{p,1} \times \hat{S}_1 & {}^{w}R_p \cdot \hat{r}_{p,2} \times \hat{S}_2 & {}^{w}R_p \cdot \hat{r}_{p,3} \times \hat{S}_3 & \hat{U}_1 & \hat{U}_2 & \hat{U}_3 \end{bmatrix}^T \tag{34}$$

This result corroborates that reported in [34], and accords with the work of Ciblak and Lipkin [29] (in this work the authors develop a model of a rigid body connected to the ground by springs. For the 3-UPU robot, the model consists of three linear springs and three torsional springs in parallel, which resembles J). Observing J, one can detect that the rows of J (the columns of Eq. (34)) are all lines lying on the *Klein quadric* M_2^4, as they satisfy Klein's equation [27,35,25]:

$$p_{01}p_{23} + p_{02}p_{31} + p_{03}p_{12} = 0 \tag{35}$$

Next, we investigate J in the robot base configuration. The investigation is based on the LCAA method presented in section 2. For simulation we take $P = [0,0,60]$ (the location of the center point of the moving platform), and equal limb lengths as follows:

$r_b = 20$ units
$r_p = 10$ units
radii of base and moving platforms

Limbs are equally placed every 120 deg, both in the base and at the moving platform.

Results:. The three linear complexes are:

$$A1 = [-0.9382 \;\; 0.3460 \;\; 0.0000 \;\; -34.5987 \;\; -93.8239 \;\; 0.0000]$$

$$A2 = [0.3460 \;\; 0.9382 \;\; 0.0000 \;\; -93.8239 \;\; 34.5987 \;\; 0.0000]$$

$$A3[0.0000 \;\; 0.0000 \;\; 1.0000 \;\; 0.0000 \;\; 0.0000 \;\; 0.0000]$$

where

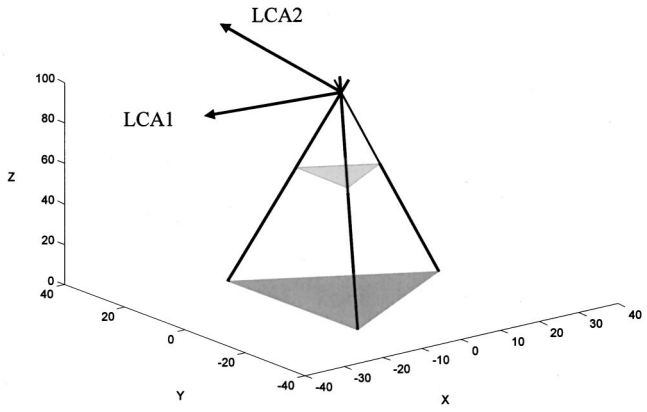

Fig. 10 3-UPU with two zero-pitch linear complexes

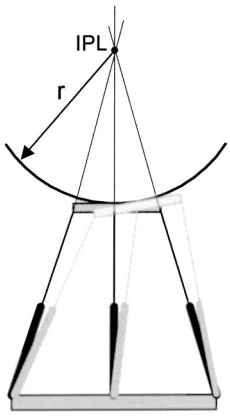

Fig. 11 The path of the moving platform on a sphere centered at IPL

$$\lambda_1 = 0, \quad \lambda_2 = 0, \quad \lambda_3 = 3$$

using (11), one obtains:

$$\sigma_1 = 0, \quad \sigma_2 = 0, \quad \sigma_3 = 1.7321$$

and from (13), the pitch is:

$$\text{Pitch}_1 = 0, \quad \text{Pitch}_2 = 0, \quad \text{Pitch}_3 = 0$$

4.1 Discussion: Simulation Results of the 3-UPU Manipulator. Applying the method of the closest linear complex on the 3-UPU robot in its zero position ($P=[0,0,p_z]$), the lines of J (Eq. (34)) are contained in two zero-pitch linear complexes, C_1 and C_2, passing at the intersection point of the extension of the three limbs of the actuator (see Fig. 10). The intersection of $C_1 \cap C_2$ defines a two-parameter family of lines: a congruence. This result implies that the robot gains an instantaneous two-parameter rotational motion about any horizontal axes passing through the intersection point of the robot limbs. These axes are the linear combination of the two zero-pitch screws as they define a plane pencil whose vertex is the intersection point of the limbs.

This result agrees with the results presented by in [36], who introduced a new type of singularity which they call *constraint singularity*. For the SNU 3-UPU robot the constraint that each leg imposes on the mobile platform, when the latter has the same orientation as the base, is that the platform may not rotate about an axis normal to the two parallel *U*-joint planes. In the case presented, the system of the constraining wrenches of the mechanism consists of only one screw, which is the vertical moment. Hence, the twist system of the platform is a five-system and the mechanism gains a two-system of all rotations with horizontal axes through the legs' intersection point. For further information regarding *constraint singularity* and its application, see [37].

When the robot moves near its base configuration (Figs. 11–16), it is no longer in a singular configuration. The following simulation presents the robot's motion on a sphere centered at the original intersection of the limbs, and calculates the closest linear complexes. Observing equations (4) and (10), one can detect that.

$$F(X) = \sum_{i=1}^{k} (\overline{x} \cdot l_i + x \cdot \overline{l_i})^2 = \chi^T M \chi = \lambda$$

Hence, λ has the meaning of the sum of square of the mutual moment of the lines L_i with respect to C. Another interpretation of λ is of the sum of the square of the virtual work generated by the structure to the platform, when the latter is moving instantaneously in the twist direction given by χ.

Equation (11), which describes the standard deviation of the lines L_i from C, may now be written as:

$$\sigma = \sqrt{\frac{\lambda}{k-5}} = \sqrt{\frac{\sum_{i=1}^{k} m(L_i, C)^2}{k-5}}$$

which is the sum of the square of error from L_i to C.

In the previous simulation of the 3-UPU robot, we saw that while in base configuration $P=[0,0,60]$, the robot gains an instantaneous two-parameter rotational motion about any horizontal axis passing through the intersection point of the robot's limbs. This means that the robot can rotate instantaneously around the intersection point of the limbs (IPL). This motion can be described as a set of points, reachable by the robots' platform, placed on a

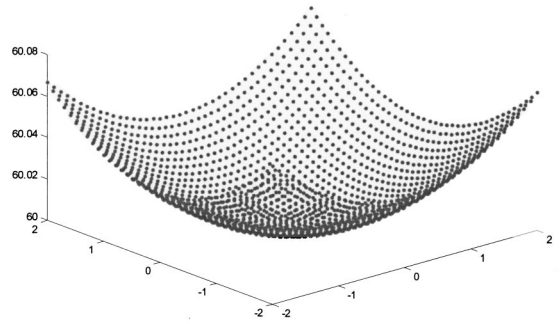

Fig. 12 Points in the vicinity of the base configuration, on a sphere centered at IPL

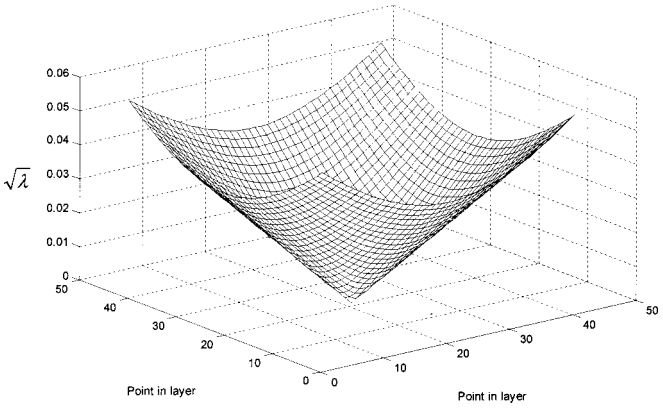

Fig. 13 Minimum $\sqrt{\lambda}$ corresponding to two LCA in points of Fig. 12

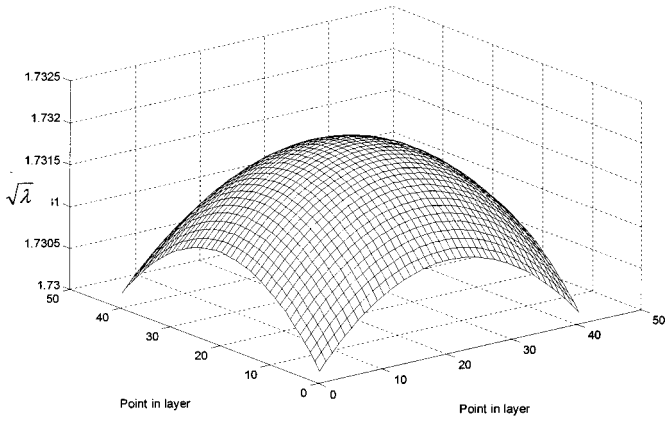

Fig. 14 Maximum $\sqrt{\lambda}$ at each point of Fig. 12

sphere centered at the IPL with a radius of IPL-P. Note that the platform is tangent to the sphere at the given points (Fig. 11). Taking all the above into consideration, a new simulation was performed in the vicinity of the base configuration point (0.14 m×0.14 m), forming a patch of a sphere. In each point, the LCAA was applied. The results are given next:

It can be seen that the robot is no longer in a singular position. However, there are still two linear complexes with low σ values, (0.05 and 0) at base configuration. These results, together with the

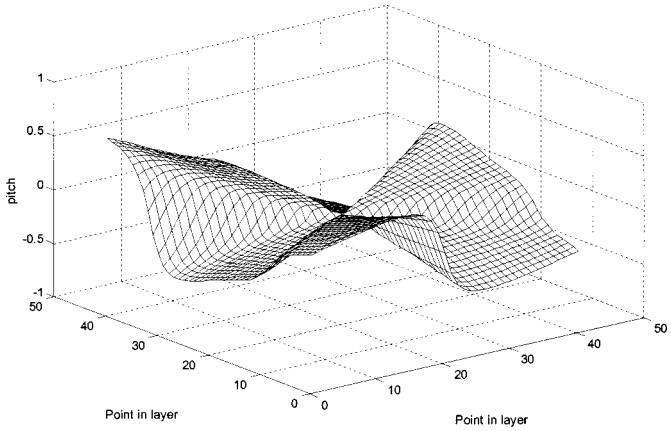

Fig. 15 Two pitches corresponding to the two linear complexes with minimum $\sqrt{\lambda}$ at each point of Fig. 12

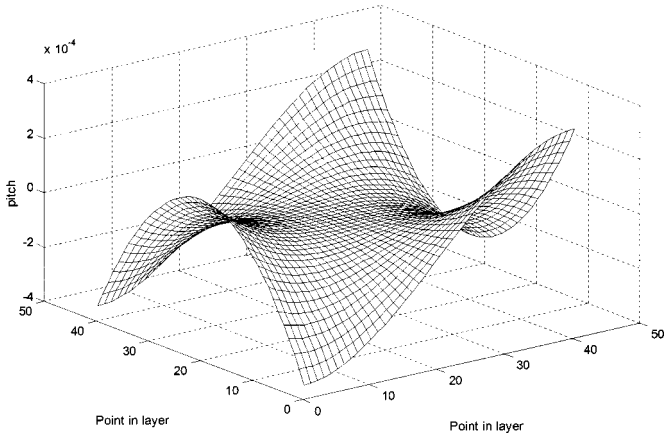

Fig. 16 Pitch of linear complex with max $\sqrt{\lambda}$ at each point of Fig. 12

interpretations of m, σ and p, indicate the possibility of an uncontrolled motion of the platform. This movement can occur when manufacturing tolerances are greater than the value of σ.

Conclusions

This investigation presents a method for analyzing the type of singularity and the behavior of parallel manipulators while at these singular configurations. The method is based on minimization of the moment of the set of governing lines with respect to a linear complex. One, two or three linear complexes that fit the set of governing lines (a linear complex, congruence, and a regulus, respectively) are possible. In these cases the robot has an instantaneous mobility of one, two, or three parameters respectively (except for spherical links, where it can move only in two directions, Merlet [1]).

Various known examples, such as Hunt's and Fichter's singularities, along with a few selected examples taken from Merlet's work [1] were presented and analyzed using the presented method.

The method was also used to investigate the singularity phenomena of the 3-UPU manipulator. Deriving the 6×6 matrix of governing lines of the three DOF 3-UPU manipulator in its base configuration, reveals that the matrix is singular. Moreover, by using the linear complex approximation it was found that the lines of this matrix are fitted by two axes with zero-pitch linear complexes (linear congruent). This result implies that the robot gains an instantaneous mobility of a two-parameter motion. This motion is a pure rotation about any screw axis, which belongs to the flat pencil, defined by the two axes of the linear complexes. When the robot deviates from this singular configuration along a sphere centered at the intersection of the limbs, the matrix's lines remain close to two linear complexes with low values of σ. Practically, this still allows two uncontrolled motions of the moving platform due to manufacturing tolerances.

References

[1] Merlet, J. P., 1992, "Singular Configurations of Parallel Manipulators and Grassmann Geometry," Int. J. Robot. Res., **8**(5), pp. 45–56.
[2] Hunt, K. H., 1983, "Structural Kinematics of In-Parallel-Actuated Robot Arms," ASME J. Mech. Des., **105**(4), pp. 705–712.
[3] St-Onge, B. M., and Gosselin, C. M., 2000, "Singularity Analysis and Representation of the General Gaugh-Stewart Platform," Int. J. Robot. Res., **19**(3), pp. 271–288.
[4] Dasgupta, B., and Mruthyunjaya, T. S., 1998, "Singularity-Free Path Planning for the Stewart Platform Manipulator," Mech. Mach. Theory, **33**(6), pp. 711–725.
[5] Gosselin, C., and Angeles, J., 1990, "Singularity Analysis of Closed-Loop Kinematic Chains," IEEE Trans. Rob. Autom., **6**(3), pp. 281–290.
[6] Zlatanov, D., Fenton, R. G., and Benhabib, B., 1994, "Singularity Analysis of Mechanisms and Robots via a Motion-Space Model of the Instantaneous Kinematics," *Proceedings of the IEEE International Conference on Robotics and Automation*, Vol. 2, pp. 980–991.
[7] Ma, O., and Angeles, J., 1992, "Architecture Singularities of Parallel Manipulators," Int. J. Robot. Res., **7**(1), pp. 23–29.
[8] Mohammadi Daniali, H. R., Zsombor-Murray, P. J., and Angeles, J., 1955, "The Isotropic Design of Two General Classes of Planar Parallel Manipulators," J. Rob. Syst., **12**(2), pp. 795–805.
[9] Zlatanov, D., Fenton, R. G., and Benhabib, B., 1995, "A Unifying Framework for Classification and Interpretation of Mechanism Singularities," ASME J. Mech. Des., **117**, pp. 566–572.
[10] Mayer St-Onge, B., and Gosselin, C. M., 1996, "Singularity Analysis and Representation of Spatial Six-Degree of Freedom Parallel Manipulator," *Advances in Robot Kinematics* (ARK), J. Lenarcic and V. Parenti-Castelli, eds., Kluwer Academic Publisher, pp. 389–398.
[11] Sefrioui, J., and Gosselin, C. M., 1995, "On the Quadratic Nature of the Singularity Curves of Planar Three-Degree-of-Freedom Parallel Manipulators," Mech. Mach. Theory, **30**(4), pp. 533–551.
[12] Collins, C. L., and McCarthy, J. M., 1998, "The Quartic Singularity Surface of Planar Platforms in the Clifford Algebra of the Projective Plane," Mech. Mach. Theory, **33**(7), pp. 931–944.
[13] Feng-Cheng, Y., and Haug, E. J., 1994, "Numerical Analysis of the Kinematic Working Capability of Mechanisms," ASME J. Mech. Des., **116**, pp. 111–117.
[14] Funabashi, H., and Takeda, Y., 1995, "Determination of Singular Points and Their Vicinity in Parallel Manipulators Based on the Transmission Index," *Ninth World Congress on the Theory of Machines and Mechanisms*, pp. 1977–1981.
[15] Karger, A., and Husty, M., 1996, "On Self-Motion of a Class of Parallel

Manipulators,'' *Advances in Robot Kinematics*, J. Lenarcic and V. Parenti-Castelli, eds., Kluwer Academic Publisher, pp. 339–348.
[16] Karger, A., 1998, ''Architecture Singular Parallel Manipulators,'' *Advanced in Robot Kinematics: Analysis and Control*, J. Lenarcic and M. L. Husty, eds., Kluwer Academic Publisher, pp. 445–454.
[17] Merlet, J. P., 1989, ''Parallel Manipulators Part 2: Theory, Singular Configurations and Grassmann Geometry,'' Rapport de Recherche INRIA No 791, F'evrier.
[18] Merlet, J. P., 1992, ''On the Infinitesimal Motion of a Parallel Manipulator in Singular Configurations,'' *IEEE Int. Conf. on Robotics and Automation*, pp. 320–325, Nice, France.
[19] Fichter, E. F., 1986, ''A Stewart Platform-Based Manipulator: General Theory and Practical Construction,'' Int. J. Robot. Res., **5**(2), pp. 155–182.
[20] Collins, C. L., and Long, G. L., 1995, ''The Singularity Analysis of an In-Parallel Hand Controller for Force-Reflected Teleoperation,'' IEEE Trans. Rob. Autom., **11**(5), pp. 661–669.
[21] Dandurand, A., 1984, ''The Rigidity of Compound Spatial Grid,'' Structural Topology, **10**, pp. 41–55.
[22] Ben Horin, R., 1997, ''Criteria for Analysis of Parallel Robots,'' Doctoral Dissertation, Technion-Israeli Institute of Technology.
[23] Simaan, N., and Shoham, M., 2001, ''Singularity Analysis of a Class of Composite Serial In-Parallel Robots,'' IEEE Trans. Rob. Autom., **17**(3), pp. 301–311.
[24] Hao, F., and McCarthy, J. M., 1998, ''Conditions for Line-Based Singularities in Spatial Platform Manipulators,'' J. Rob. Syst., **15**(1), pp. 43–55.
[25] Hunt, K. H., 1978, ''Kinematic Geometry of Mechanisms,'' Department of Mechanical Engineering, Monash University, Clayton, Victoria, Australia.
[26] Pottmann, H., Peternell, M., and Ravani, B., 1999, ''An Introduction to Line Geometry With Applications,'' Comput.-Aided Des., **31**, pp. 3–16.
[27] Klein, F., 1871, ''Uber Liniengeometrie und Metrische Geometrie,'' Mathematische Annalen, pp. 257–303.
[28] Ball, R. S., 1900, *A Treatise on the Theory of Screws*, Cambridge University Press, Cambridge.
[29] Ciblak, N., and Lipkin, H., 1999, ''Synthesis of Cartesian Stiffness for Robotic Applications,'' *Proceedings of the 1999 IEEE International Conference on Robotics and Automation*, Detroit, Michigan., pp. 2147–2152.
[30] Tsai, L.-W., and Joshi, S., 2000, ''Kinematics and Optimization of a Spatial 3-UPU Parallel Manipulator,'' ASME J. Mech. Des., **122**(4), pp. 439–446.
[31] Tsai, L.-W., 1996, ''Kinematics of a Three-DOF Platform With Three Extensible Limbs,'' Advances in Robot Kinematics (ARK), J. Lenarcic and V. Parenti-Castelli, eds., Kluwer Academic Publisher, pp. 401–410.
[32] Di Gregorio, R., and Parenti-Castelli, V., 2002, ''Mobility Analysis of the 3-UPU Parallel Mechanism Assembled in a Pure Translational Motion,'' ASME J. Mech. Des., **124**, pp. 259–264.
[33] Tsai, L.-W., 1998, ''The Jacobian Analysis of a Parallel Manipulator Using Reciprocal Screws,'' Advances in Robot Kinematics (ARK): Analysis and Control, Lenarcic, J., and Husty, M. L., eds., Kluwer Academic Publishers, pp. 327–336.
[34] Parenti-Castelli, V., Di Gregorio, R., and Bubani, F., 2000, ''Workspace and Optimal Design of a Pure Translation Parallel Manipulator,'' Meccanica **35**, pp. 203–214; (anche presentato al 14th Italian Congress on Theoretical and Applied Mechanics AIMETA, Como, Italy, October 6–9, 1999).
[35] Sommerville, D. M. Y., 1934, *Analytical Geometry of Three Dimensions*, Cambridge University press.
[36] Bonev, I., and Zlatanov, D., 2001, ''The Mystery of the Singular SNU Translational Parallel Robot,'' http://www.parallemic.org/Reviews/Review004.html.
[37] Zlatanov, D., Bonev, I., and Gosselin, C., 2001, ''Constraint Singularities as Configuration Space Singularities,'' http://www.parallemic.org/Reviews/Review008.html.